Available online at www.sciencedirect.com
SCIENCE DIRECT®
Polymer 45 (2004) 3139–3147
polymer
www.elsevier.com/locate/polymer

Role of interfacial adhesion strength on toughening polypropylene with rigid particles

Y.S. Thio*, A.S. Argon, R.E. Cohen

Department of Chemical Engineering and Department of Mechanical Engineering, Massachusetts Institute of Technology, Cambridge, MA 02139, USA

Received 10 September 2003; received in revised form 13 February 2004; accepted 19 February 2004

Abstract

The effects of interfacial adhesion strength on the mechanical properties of composites of polypropylene and glass particles were investigated. The 3.5 μm average diameter glass particles were surface-treated using two silanes with different functional groups. The functional groups were hydrocarbons, expected to promote adhesion between filler and matrix, and fluorocarbons, expected to reduce the strength of adhesion. Mixtures of the functional groups were also used to treat the surface of the glass to obtain better control of adhesion strength and thus the mechanical properties of the composites. A model study using glass slides and polypropylene films was conducted to confirm the feasibility of treatment. Adhesion strength between glass and polypropylene increased with increasing coverage of the hydrocarbon silanes. The surface-modified particles were incorporated into the polypropylene matrix via melt processing. While surface functionalization of the particles can influence the dispersion of the particles, no significant effect was observed in this study. Tensile tests and toughness tests were performed on injection-molded samples. The tensile strength of the reinforced polypropylene increased with increasing adhesion strength. Impact toughness increased with weaker adhesion but the dependence became less pronounced as deformation rate was increased.

Keywords: Polypropylene; Rigid particle toughening; Debonding

1. Introduction

The interface between inorganic filler particles and the matrix polymer plays an important role in determining the properties of a composite. Particle–matrix interaction is expected to influence the structure of the composites, mainly through its influence on the dispersion of the filler particles in the matrix. The interfacial strength is also expected to affect local processes occurring during macroscopic deformation of the composites. One important process thus affected in these particulate composites is the debonding process, which is the separation of the filler particles from the matrix during deformation [1–3]. Previous works have shown that debonding is an important mechanism in promoting toughness of particulate-filled polymers because it allows the plastic stretch of polymer ligaments between the debonded particles [4–6]. The work presented here makes the connection between the interfacial strength and the toughness of polymer–inorganic composites by investigating the role of the interfacial strength in the evolution of morphology (debonding) and the macroscopic mechanical properties.

The polymer–inorganic interface can be tuned most readily by modifying the surfaces of the particles. Physical modification of the filler surfaces, e.g. changing the surface roughness, is possible [7] but more costly and hence less commonly performed than chemical treatment methods. Most commonly, the surface is treated to become more chemically compatible with the polymer matrix. Hence, the molecules used in these treatments are typically amphoteric surfactant molecules. The chemical treatment of the surfaces of inorganic fillers can be classified into two broad categories based on the interaction between the surfactant and the inorganic particles: non-reactive treatment and reactive treatment [8]. Non-reactive treatment methods typically utilize molecules with polar hydrophilic groups that associate with the inorganic fillers while the

* Corresponding author. Present address: Chemical Engineering and Materials Science Department, University of Minnesota, 151 Amundson Hall, 421 Washington Avenue SE, Minneapolis, MN 55455, USA. Tel.: +1-612-626-1005; fax: +1-612-626-1686.
E-mail address: thio@alum.mit.edu (Y.S. Thio).

0032-3861/$ - see front matter © 2004 Elsevier Ltd. All rights reserved.
doi:10.1016/j.polymer.2004.02.064

hydrophobic groups interact with the polymer matrix; the interactions are van der Waals and polar–polar forces. In reactive treatment methods, one end of the surfactant molecules reacts with the inorganic surface to produce covalent bonds, which are stronger than the non-bonded interactions in the non-reactive treatment case. A very common reactive treatment is the silane treatment of glass fibers and beads. As an example of the reaction, chlorosilanes can react with glass surfaces under aprotic conditions, i.e. in solvents such as toluene and xylene, through direct nucleophilic reaction of the silanol group on the glass surface with the chlorines [9]. The widespread use of the silane treatment can be attributed to the availability of a wide range of endgroups. Thus, the interaction between the inorganic surface and the matrix polymer can be tuned by selecting the appropriate endgroups.

The interaction strength at the interface can be estimated quantitatively by the work of adhesion [10]:

$$W_{AB} = \gamma_A + \gamma_B - \gamma_{AB} \quad (1)$$

where W_{AB} is the work of adhesion of two surfaces A and B, γ_A and γ_B the surface energies of surface A and surface B, and γ_{AB} the interfacial energy (usually modeled as some combination of γ_A and γ_B). The work of adhesion between the polymer matrix and the inorganic fillers in a composite is a reasonable indicator for certain macroscopic properties of the composite. For instance, some studies have reported a linear positive relationship between tensile strength of PP/$CaCO_3$ composites and the work of adhesion [8].

Several facile methods, such as peel tests [11] and double cantilever beam tests [12], have been developed to evaluate the adhesion strength between polymeric and inorganic surfaces when the surfaces are relatively large and have low radii of curvature. The direct evaluation of the adhesion strength in composites is less straightforward because of the more complex geometry and the statistical scatter due to imperfect surfaces and non-uniform particle size. In fiber composites, tests such as the fiber fragmentation test [13] and the single fiber pull-out test [14] have been developed. Analogous to these, for composites based on particulate fillers, some single-particle studies have been demonstrated [15,16]. Another approach in characterizing the adhesion between the inorganic fillers and the polymer matrix is to determine the onset of the debonding process during deformation: the stronger the adhesion, the higher is the stress or strain required for debonding to occur. Methods to determine the onset of debonding include the acoustic emission method [17,18] and the tensile dilatometry method [19]. The work presented here makes use of the latter method.

This work focuses on the study of composites of polypropylene (PP) and surface-modified glass particles, in particular investigating the adhesion between the two phases, the debonding process during the deformation of the composites, and the resulting mechanical properties. The surface treatment used two types of silane molecules: one with hydrocarbon functional group and one with fluorocarbon group. These molecules were chosen because of the difference in the expected surface energies of the treated substrates due to the fluorocarbon and the hydrocarbon endgroups. Fluorocarbon surface treatment is often used to create low energy surfaces while hydrocarbon endgroups are used in coupling agents that interact well with polyolefins such as PP. As a model system to study the interaction between PP and silane-functionalized glass, planar PP and glass surfaces were used. This model study was then extended to the real system of interest, namely composites of PP and spherical glass particles, where an investigation was performed on the role of interfacial strength on the debonding process and the toughness of the composites.

2. Experimental

2.1. Polypropylene and planar glass as model systems

The polypropylene used in this study was Accpro 9346 from BP Amoco Polymers, Inc. Glass microscope slides of 2 mm thickness were purchased from VWR Scientific Inc. Two types of silanes were used for surface treatment, heptadecafluorodecyl trichlorosilane ('CF-silane') and *n*-decyl trichlorosilane ('CH-silane'), obtained from Gelest Inc. The structures of these silanes are given in Fig. 1.

Silane treatment solutions were made by dissolving 0.1 vol% silane in *p*-xylene, purchased with 99 + % purity from Aldrich Chemical Co., Inc. Mixtures of the silane were used to create solutions varying from 100% CF-silane to 100% CH-silane. The glass slides were cleaned in a base bath (5 wt% NaOH in a solution of 50–50 vol% water and ethanol) then immersed for 12 h at room temperature in the silane solution, which was kept well-mixed with a magnetic stir bar. The slides were rinsed using pure xylene, dried using nitrogen flow, and cured in a vacuum oven at 100 °C for 2 h.

2.2. Characterization of treated glass surfaces

To characterize the thickness of the silane layers,

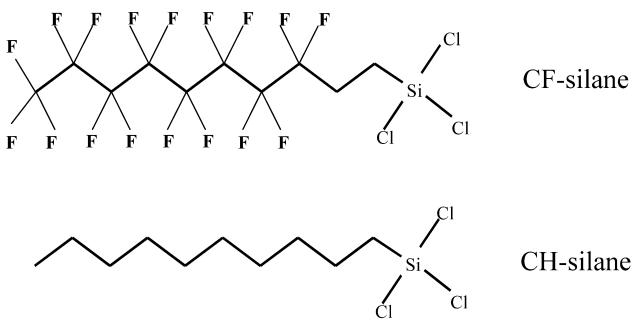

Fig. 1. The two silanes used in this work: heptadecafluorodecyl trichlorosilane ('CF-silane') and *n*-decyl trichlorosilane ('CH-silane').

ellipsometry was performed on silane-treated pieces of silicon wafer. The wafers were purchased from Exsil Inc. The exposed silicon layer was the (100) plane with a native oxide (SiO_2) layer. Silicon wafers were used instead of glass slides in this study because ellipsometry requires non-transparent substrates. The surface energies of the treated glass surfaces were measured using the Zisman plot construction [20]. A homologous series of liquids was chosen: *n*-decane, *n*-dodecane, *n*-hexadecane, *n*-octadecane. The solvents used in this experiment were obtained from Aldrich Chemical Co. Inc. The advancing contact angles of these liquids on each glass surface of interest were measured.

The adhesion between polypropylene and the surface-modified glass surfaces was characterized by a stud-pull test on a Sebastian I materials tester machine from Quad Group Inc. The test complies with Mil. Std. 883 Method 2027. Polypropylene was spin-coated from a 120 °C xylene solution on the surface-modified glass slides. The coating process was done at 100 rpm for 1 min. The thickness of the coated polypropylene layer was 0.50 ± 0.05 μm as measured by profilometry. A nail-shaped stud with a diameter of 1.5 mm coated by a 0.1 in. thick uncured epoxy was physically attached to the polypropylene surface. The samples were then cured in the vacuum oven at 125 °C for 2 h to bond the stud onto the polypropylene. Each sample was placed in the peel-test machine, and the pin was pulled down at 0.1 mm/s. The machine recorded the force required to completely tear away the polypropylene from the silanized glass surface.

2.3. Composites of polypropylene and glass particles

The same polypropylene batch (Accpro 9346 from BP Amoco Polymers, Inc.) was used in making the polypropylene-glass particle composites. The filler particles were spherical glass (Spheriglass 10000E) with an average diameter of 3.5 μm from Potters Industries Inc. The glass particles were treated in a similar way as the glass slides described in the previous section. First they were suspended in a stirred base bath (5 wt% NaOH in 50–50 vol% water and ethanol) to clean the surfaces from organics. The particles were then separated by vacuum filtration, dried, and then put into suspension in the silane treatment solution described in the previous section. The amount of the silane added in the solution was calculated to yield a monolayer of silane on the glass surface, assuming a uniform diameter of 3.5 μm for the glass particles, a surface area of 50 $Å^2$ for each silane molecule, and complete reaction of all the silanes [9]. The suspension was stirred for 12 h. The particles were then dried again using vacuum filtration and heat-treated in a vacuum oven at 100 °C for 2 h. Three silane treatment solutions were used: a solution containing only CF-silane (labeled as CF), one with only CH-silane (labeled CH), and one containing a 50–50 vol% mixture of CH and CF (labeled CH + CF). The glass particle surfaces were examined using X-ray photoelectron spectroscopy (XPS) for identification of elements on the surfaces, using an Axis Ultra XPS from Kratos, with 1486.6 eV beam from a magnesium source.

The glass particles were compounded with the PP using MicroCompounder, a mini co-rotating twin-screw extruder from DACA Inc. The extruder was operated at 190 °C and 100 rpm screw rotation rate. Each sample had a residence time of 3 min inside the extruder. Composites with 10 vol% glass in PP were made. The mixture was injection molded into samples using MicroInjector from DACA Inc. The injection temperature was 200 °C whereas the mold was at room temperature. The composites were molded into tensile dogbones with the dimensions of deformable region being 25.0 mm × 4.1 mm × 1.5 mm and into rectangular bars for toughness tests with dimensions of 63.5 mm × 10.2 mm × 3.2 mm. The bars were subsequently notched at the middle of the longest dimension using a TMI cutter to produce notches with radius 0.254 mm and depth of 2.54 mm.

2.4. Characterization of mechanical properties

Tensile tests were performed on the dogbone samples using an Instron 4201 testing machine at room temperature and at a constant crosshead speed of 15 mm/min. Three specimens were tested for each composite. Izod fracture test was carried out to characterize the impact toughness of the composites. The test was performed at room temperature using a Tinius Olsen 892 impact test machine with pendulum speed at impact of 3.46 m/s. Toughness tests were also performed on the composites at a slower rate than impact condition by uniaxial tensile deformation of the notched rectangular bar samples. The tests were performed on an Instron 4201 testing machine at room temperature and with a crosshead speed of 15 mm/min. For the toughness tests, four specimens were tested for each composite.

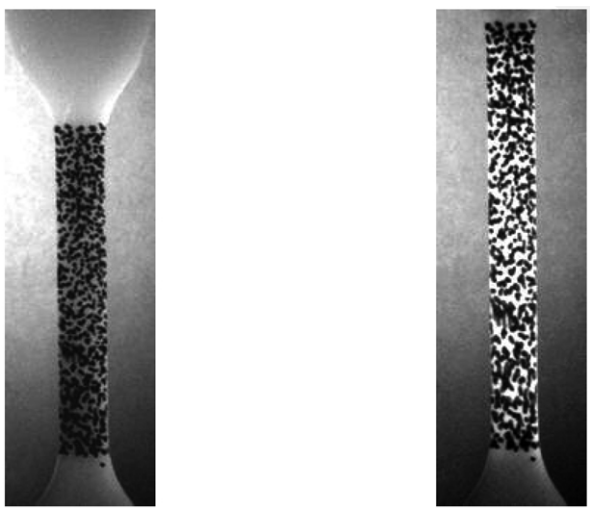

Fig. 2. The speckle pattern used in the optical tensile dilatometry experiment, before and after deformation.

2.5. Measuring debonding in composites of polypropylene and surface modified glass particles

To measure the onset of debonding during the deformation of the PP-glass composites, tensile dilatometry experiments were performed [19]. The strains were measured through an optical method. On the surface of each sample, a speckle pattern was created using a permanent marker; a typical pattern is shown in Fig. 2. Comparison of the position of each placed mark and its proximity to neighboring marks at different time points yields a measure of the local strain. Uniaxial tensile tests were performed on the samples using an Instron 5582 testing machine at a constant crosshead speed of 15 mm/min. During each run, digital video images of the speckle pattern were taken at a regular interval. Image analysis on the captured images using Vic-2D Digital Image Correlation software (Correlated Solutions, Inc.) produced local strain maps in both the axial and the transverse directions. Assuming lateral isotropy, the volumetric strain can be approximated as:

$$\frac{\Delta V}{V_o} = (1+\varepsilon_1)(1+\varepsilon_2)^2 - 1 \quad (2)$$

where ΔV is the change in volume, V_o the original volume, ε_1 the axial strain, and ε_2 the lateral strain. Thus, maps of local volumetric strains were obtained for each sample. Average values of volume strain for the entire sample were also calculated.

3. Results and discussion

3.1. Adhesion between polypropylene and treated glass surface

The thickness of the silane layers on the glass slides as measured by ellipsometry was 30–50 Å. Assuming fully extended endgroups with a length of ~15 Å, the measured thickness corresponds to 2–3 monolayers of silane on the surface, indicating some incomplete reaction to the glass surface and folding of the silane molecules on the surface.

In constructing the Zisman plot to characterize the critical surface energy of these surfaces, the cosines of measured contact angles of a series of liquids on these surfaces were plotted against the surface tension of the liquids. At room temperature, the surface tension of *n*-octane, *n*-decane, *n*-dodecane, *n*-hexadecane, and *n*-octadecane are 23.4, 24.9, 27.0, and 27.9 mJ/m^2, respectively. An example of the Zisman plot is given in Fig. 3. A linear extrapolation of the trend to the *x*-axis ($\cos\theta = 1$) yields the critical surface energy γ_c as the intercept, which is a good approximation of the surface energy of the solid surface, γ_S.

Performing the procedure described above on a series of surface-modified glass slides yields Fig. 4, showing the effect of silane composition on the surface energy of the

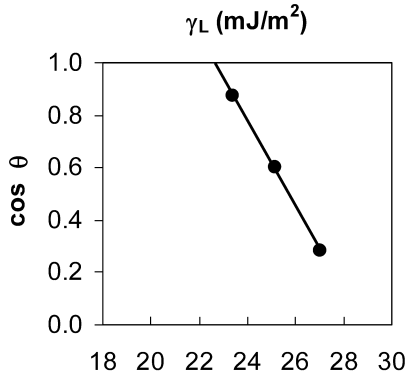

Fig. 3. An example of the Zisman plot construction to determine the surface energy of a solid surface. The solid surface is a glass slide treated with 60% CF-silane and 40% CH-silane solution. The liquids used are *n*-decane, *n*-dodecane, and *n*-hexadecane.

treated glass. Note that there is no value reported for the γ_c of the glass surface treated with 100% CH-silane solution. This is because that particular surface is wetted completely by all the liquids used in this experiment; therefore the Zisman construction cannot be performed. Nevertheless, it can be concluded that γ_c of that surface is larger than 28 mJ/m^2 (the surface energy of *n*-octadecane, the liquid used with the highest surface energy).

This result demonstrates that, as expected, the higher the CF-silane concentration in the treatment solution, the lower is the surface energy of the treated surface. Assuming that γ_c approximates the surface energy of the solid surface, the theoretical value of the work of adhesion between these treated glass surfaces and PP can be estimated using Eq. (1). This will yield a similar trend as shown in Fig. 4, i.e. higher amount of CF-silane treatment produces lower work of adhesion between the treated glass and PP. While the trend from this purely surface energetic consideration can be expected to be reflected in macroscopic measurements of adhesion, the exact values will be affected by sample geometry, surface roughness, and processes at the molecular level such as the entanglement of the CH-endgroups with the polymer chains.

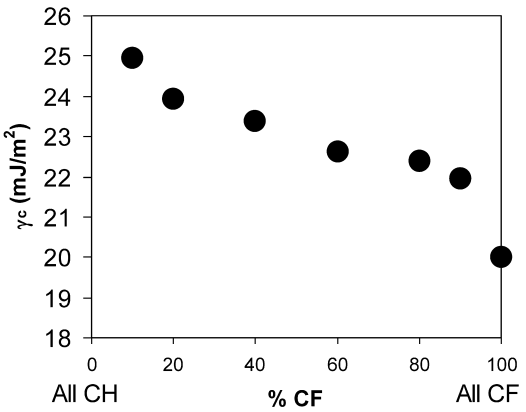

Fig. 4. Surface energy of surface-modified glass surface. On the horizontal axis is the amount of CF silane in the solution used to treat the glass slide.

The adhesion strength between polypropylene and the treated glass surfaces as characterized by the stud-pull test is reported in Fig. 5. As expected, surfaces with more CF-silane treatment adhere less strongly with polypropylene. This observation is consistent with the surface energy measurements shown in Fig. 4, which show that higher CF-silane content in the treatment solution led to lower surface energy of the treated glass.

3.2. Surface modification of glass particles

X-ray photoelectron spectroscopy (XPS) was used to determine the effectiveness of the silane treatment on the micron-sized glass particles. The spectra are given in Fig. 6 where the major elements associated with the peaks are identified. Table 1 reports the calculated relative amount of elements based on the area under the peaks. Since different elements have different sensitivity factors in the XPS experiment, each peak was normalized with the corresponding relative sensitivity factor (RSF), whose values are also reported in the table.

The presence of carbon on the untreated glass samples, even after cleaning in base bath, suggests that the samples were contaminated during exposure to ambient condition. Because of this, the amount of carbon is not a good measure of the amount of silane on the surface. However, the amount of fluorine relative to silicon can be used to estimate the relative efficiency of coating of CF-silane compared to that of CH-silane. The untreated glass particles as well as those treated with 100% CH-silane solution do not contain any fluorine atoms, as can be expected. The glass particles treated with 100% CF-silane solution would be expected to have twice the amount of fluorine on the particles treated with a solution containing 50–50 mixture of CF-silane and CH-silane. However, as can be seen in the table above, the ratio of these two values is only 1.60, suggesting that the reaction rates of the two silanes are not equal. Another possible explanation is a difference in the orientation of the endgroups; larger exposure of the CH groups would cause the discrepancy between the composition of the silane

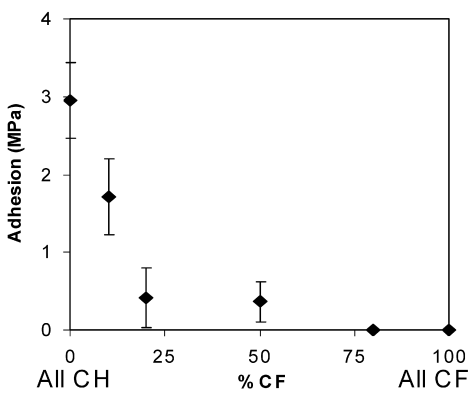

Fig. 5. Adhesion strength between polypropylene and silanized glass surface, as measured by peel test.

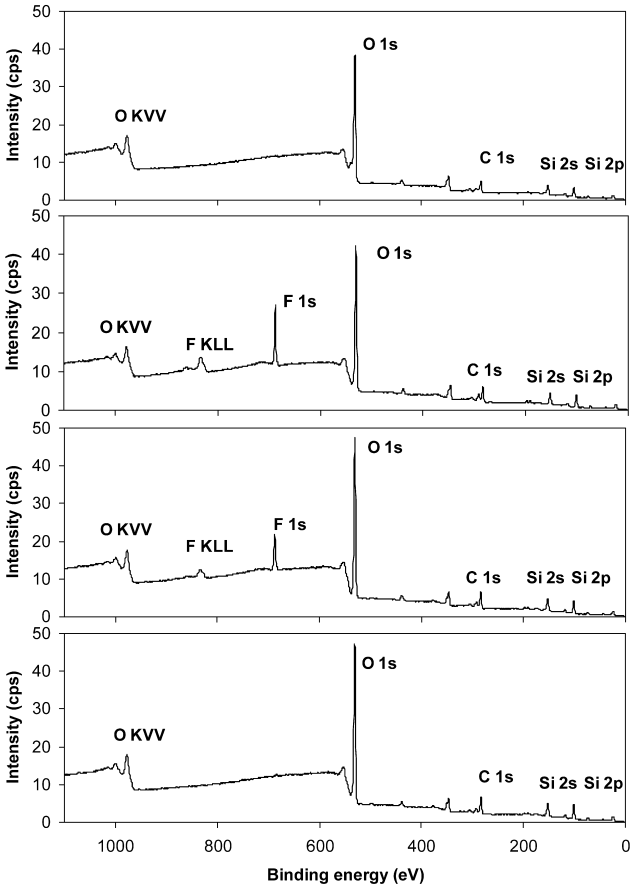

Fig. 6. X-ray photoelectron spectroscopy results for treated glass particle samples. The peaks in the vicinity of 400 eV correspond to boron and sodium (impurities in glass). The treatments are, from top to bottom: untreated; 100% CF-silane solution; 50–50 vol% CF- and CH-silane solution; 100% CH-silane solution.

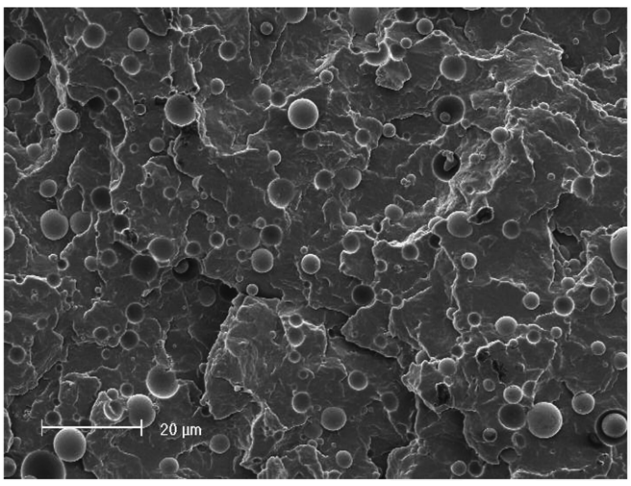

Fig. 7. SEM micrograph of a freeze-fractured sample of 10 vol% glass beads in PP showing good dispersion of the particles. The glass beads were treated using 100% CH-silane solution.

Table 1
X-ray photoelectron spectroscopy (XPS) results for the glass particles with various treatments: amounts of major elements relative to silicon (Si)

Treatment of glass particles	Si 2p (RSF = 0.33)	C 1s (RSF = 0.28)	O 1s (RSF = 0.78)	F 1s (RSF = 1.00)
Untreated	1.00	1.44	7.53	0.00
100% CF-silane	1.00	1.25	5.18	1.64
50–50% CF- and CH-silane	1.00	1.41	5.93	1.00
100% CH-silane	1.00	1.33	5.29	0.00

solution and that on the treated surface. This difference can also explain the non-linear trend of the surface energy of treated solids when plotted against the relative concentration of CF-silane and CH-silane in solution, as shown in Fig. 4. Regardless of the cause of this discrepancy, these XPS results confirm that adjusting the composition of the treatment solution results in a systematic change in the composition of CF-group and CH-group on the surfaces of the glass particles.

The different surface treatments did not appear to influence the dispersion of the glass beads in PP during melt processing. Fig. 7 is an SEM micrograph showing the dispersion of CH-silane treated glass particles in the PP matrix. This quality of dispersion was also observed in the composites formed by PP and glass beads with the other surface treatments. Likely due to the relatively large size of particles, the glass beads were well dispersed, exhibiting no aggregation or large-scale clustering.

3.3. Mechanical properties of composites of polypropylene and glass particles

The tensile stress–strain curves for the composites of PP and surface-treated glass particles are presented in Fig. 8. All the samples have a different maximum stress from that of the unfilled PP. The trend suggests a difference in the evolution of voids in these samples due to the debonding of the glass particles from the polypropylene matrix. Fig. 9 is an example of the void formation in a deformed sample. The formation of voids reduces the apparent yield stress of the composites. The varying maximum stresses in these composites (all with 10 vol% filler particles) indicates that not all particles eventually debonded in the experiments above and that lower surface energy of the particles induces more (and perhaps earlier) debonding. A more quantitative examination of the onset of debonding is discussed in the next section.

Values for Izod impact toughness of the various composites are presented in Fig. 10. The addition of glass particles and the surface modification did not affect the impact toughness significantly. The silane treatment, however, produced a difference in the slower fracture toughness test using the single edge notched bar specimen in tension. The resulting load–displacement curves are given in Fig. 11. As a qualitative measure of the toughness, the area under each load–displacement curves is given in Fig. 12. The toughness of the composites increases with increasing amount of CF-silane used in the treatment of the glass particles. This confirms the hypothesis that weaker interaction between the rigid particles and the polymer matrix will lead to higher toughness. The discrepancy between impact toughness (Fig. 10) and toughness measured in quasi-static condition (Fig. 11) indicates that the toughening process is rate dependent. It appears that during impact, the particles did not have sufficient time to debond or the interparticle ligaments of polymers were not

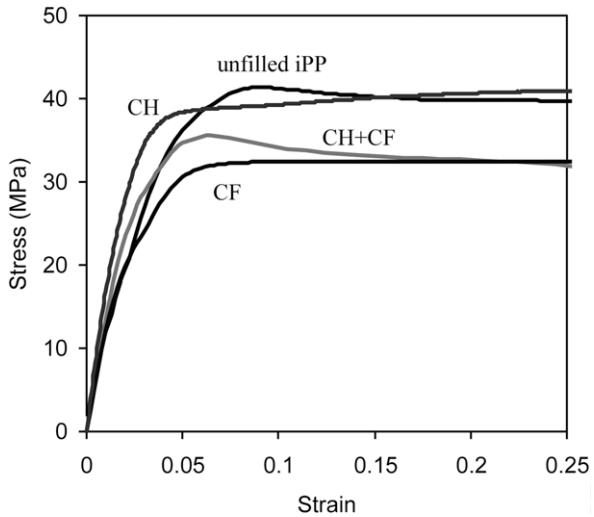

Fig. 8. Stress strain curves for composites of PP and surface-modified glass particles.

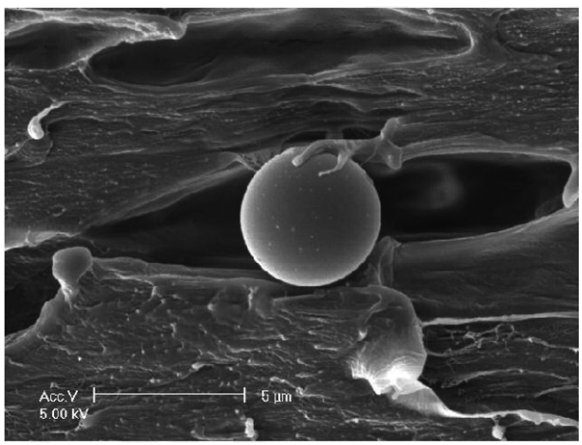

Fig. 9. Debonded glass particles surrounded by the void created due to deformation of the PP/glass composite. The glass particle was treated using CF-silane.

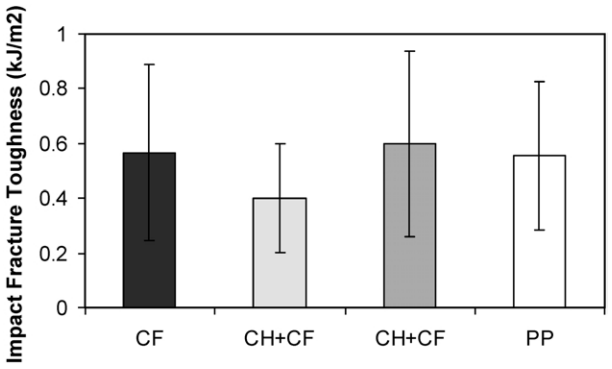

Fig. 10. Izod fracture toughness normalized by nominal fracture area. PP, unfilled PP; the others are PP + 10 vol% glass particles: CH, treated with 100% CH-silane, CH + CF, treated with 50–50 vol% CH- and CF-silane, CF, treated with 100% CF-silane.

able to deform plastically to a significant extent, as shown by the micrograph in Fig. 13.

3.4. Onset of debonding during deformation of polypropylene–glass composites

To determine the onset of debonding during the deformation of each sample, average volumetric strain over the sample was plotted against axial strain, as shown in Fig. 14.

The strain at which the slope of the volume evolution curve changes is taken to be the onset of the debonding process. Applying this method on curves such as shown in Fig. 14 yields values of strain at which the composites start to exhibit debonding. The results are summarized in Fig. 15.

Once the debonding strain is determined, the macroscopic stress at the onset of debonding can be determined from the stress–strain curves of Fig. 8. From these macroscopic stresses, the local debonding stress (the stress at the surface of the particles) can be estimated using the construction of Goodier [21,22]. Using this construction, the stress at the pole of a spherical particle embedded in a

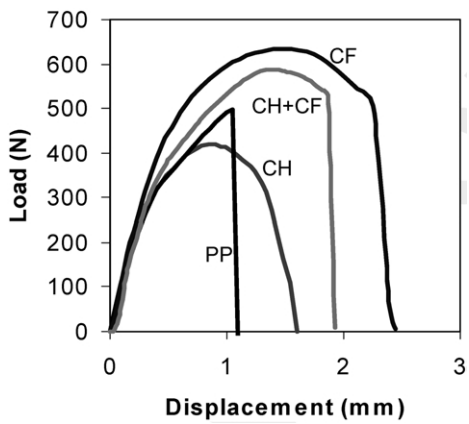

Fig. 11. Load–displacement curve from single edge notched toughness test PP, unfilled PP; the others are PP + 10 vol% glass particles: CH, treated with 100% CH-silane, CH + CF, treated with 50–50 vol% CH- and CF-silane, CF, treated with 100% CF-silane.

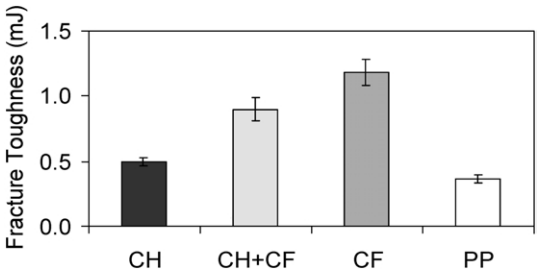

Fig. 12. Area under the load–displacement curves.

matrix of a different material is:

$$\sigma_d = \sigma_\infty(1 - A(x, \nu, \nu_p))$$

$$A = \left[\frac{x-1}{(7-5\nu)x + (8-10\nu)}\right] \times \left[\frac{(1-2\nu_p)(7-5\nu)x + 2(1+5\nu_p-5\nu\nu_p)}{(1-2\nu_p)2x + (1+\nu_p)}\right] - \left[\frac{[(1-\nu)(1+\nu_p)/(1+\nu) - \nu_p] - (1-2\nu_p)x}{(1-2\nu_p)2x + (1+\nu_p)}\right]$$

$$x = \mu/\mu_p \quad (3)$$

where σ_∞ is the applied overall tensile stress, ν the Poisson's ratio, and μ the shear modulus. The subscript p refers to the particles while unsubscripted symbols refer to the polymer matrix.

The constant A can be calculated for our system of PP matrix and glass particles, using these values for Poisson's ratio: $\nu = 0.3$ and $\nu_p = 0.24$ [23]. Since A is not sensitive to variation in x when x is small (glass being much stiffer than PP), x is taken to be 0. With these values, A is calculated to be -1.25, making the local debonding stress σ_d to be 2.25 times the applied macroscopic tensile stress σ_∞. The dependence of the debonding stress on the type of surface treatment is given in Fig. 16.

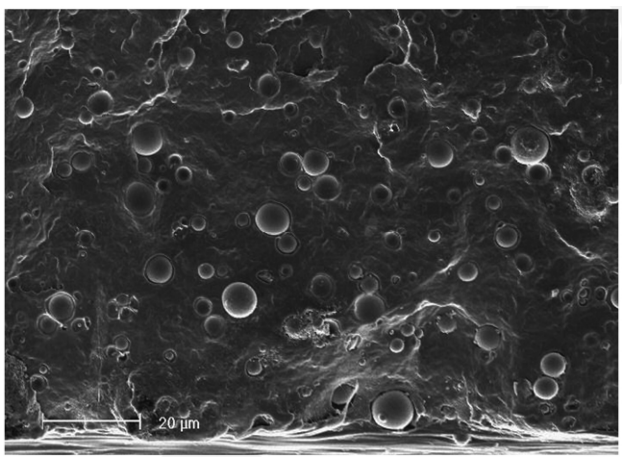

Fig. 13. SEM micrograph of fractured Izod sample of 10 vol% CH-treated glass beads in PP near the initial notch, showing little or no debonding of the particles. Fracture started at the bottom of the image and progressed upwards.

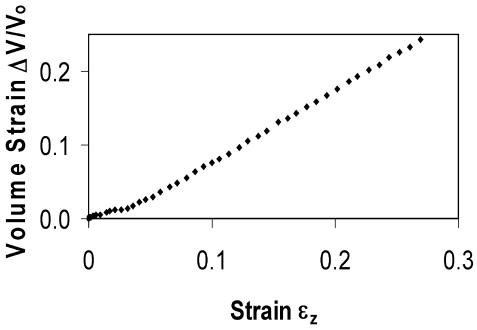

Fig. 14. Volumetric strain evolution with increasing strain for PP filled with 10% glass particles treated with CH-silane. The onset of debonding is taken to be the intersection of the lines with differing slopes.

As can be seen in the previous two figures, more CF-silane treatment leads to earlier or easier debonding. This observation agrees with the results from the study on the model system (Section 2.1), where more CF-silane treatment was shown to result in lower surface energy of the treated glass and consequently on lower work of adhesion between the glass and PP.

4. Conclusion

Higher concentration of fluorocarbon silane in the treatment solution applied on the glass particles results in weaker adhesion between the treated glass surface and PP due to the lower surface energy of fluorocarbon treated surfaces. Weaker adhesion between the rigid filler particles and the matrix polymer leads to earlier and more prevalent debonding. Earlier debonding causes more extensive amount of plasticity in the composites during deformation, which translates into significantly higher macroscopic toughness in low rate tensile experiments and no loss of toughness at high rates associated with the Izod impact test.

For the purposes of toughening, the more desirable interaction/adhesion between the filler particles and matrix polymer is a weak one. This is consistent with a toughening mechanism that requires particle–matrix debonding to facilitate the plastic stretch of the polymer ligaments between the filler particles. As indicated by the comparison of results from impact toughness tests and quasi-static toughness test, this toughening process may be strain-rate dependent. Whether the undesirable strain rate dependence depends more strongly upon the debonding mechanism itself or on the plastic deformation characteristics of the matrix polymer is an open question at this point. Studies on surface-modified glass bead filled composites with a variety of matrix polymers would help to resolve this important issue.

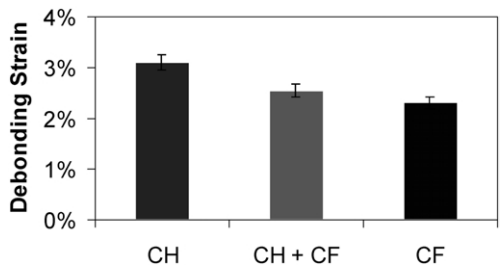

Fig. 15. The dependence of the onset of debonding on the surface treatment of the glass particles.

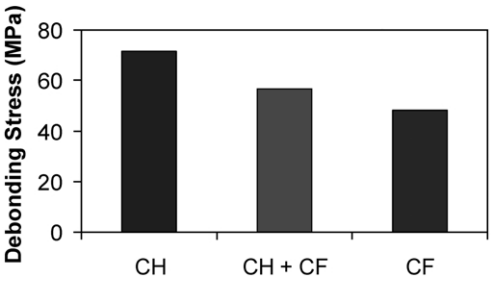

Fig. 16. The macroscopic stress at the onset of debonding and its dependence on the surface treatment of the glass particles.

Acknowledgements

This research was supported by the NSF MRSEC program through the Center of Materials Science and Engineering at MIT from Grant DMR-98-08941. We acknowledge with gratitude P.E. Laibinis and K.K. Gleason for helpful discussion.

References

[1] Pukanszky B, Fekete E, Tudos F. Makromolekulare Chemie-Macromolecular Symposia 1989;28:165–86.
[2] Jancar J, Kucera J. Polym Engng Sci 1990;30(12):707–13.
[3] Jancar J, Kucera J. Polym Engng Sci 1990;30(12):714–20.
[4] Pukanszky B, Maurer FHJ. Polymer 1995;36(8):1617–25.
[5] Thio YS, Argon AS, Cohen RE, Weinberg M. Polymer 2002;43(13):3661–74.
[6] Zuiderduin WCJ, Westzaan C, Huetink J, Gaymans RJ. Polymer 2003;44(1):261–75.
[7] Rothon RN. In: Jancar J, editor. Advances in Polymer Science, vol. 139. New York: Springer; 1999. p. 67–107.
[8] Pukanszky B, Fekete E. In: Jancar J, editor. Advances in Polymer Science, vol. 139. New York: Springer; 1999. p. 109–53.
[9] Plueddemann EP. Silane coupling agents, 3rd ed. New York: Plenum Press; 1991.
[10] Adamson AW. Physical chemistry of surfaces, 6th ed. New York: Wiley; 1997.
[11] Bonnerup C, Gatenholm P. J Adhes Sci Technol 1993;7(3):247–62.
[12] Xiao F, Hui CY, Kramer EJ. J Mater Sci 1993;28(20):5620–9.
[13] Kelly A, Tyson WR. J Mech Phys Solids 1965;13:329.
[14] Piggott MR. Load bearing composites. Boston: Kluwer Academic Publishers; 2002.
[15] Mower TM, Argon AS. J Mater Sci 1996;31(6):1585–94.
[16] Harding PH, Berg JC. J Adhes Sci Technol 1997;11(8):1063–76.
[17] Minko S, Karl A, Voronov A, Senkovskij V, Pomper T, Wilke W, Malz H, Pionteck J. J Adhes Sci Technol 2000;14(8):999–1019.
[18] Miller AC, Minko S, Berg JC. J Adhes 2001;75(3):257–66.

[19] Naqui SI, Robinson IM. J Mater Sci 1993;28(6):1421–9.
[20] Zisman WA. In: Gould RF, editor. Advances in chemistry series, vol. 43. Washington, DC: American Chemical Society; 1964.
[21] Goodier JN. Trans Am Soc Mech Eng 1933;55:39.
[22] Piorkowska E, Argon AS, Cohen RE. Macromolecules 1990;23(16): 3838–48.
[23] McClintock FA, Argon AS. Mechanical behavior of materials. Reading, MA: Addison-Wesley; 1996.